URSI GASS 2023, Sapporo, Japan, 19 – 26 August 2023

Characterization of NPF and its precursors in a semi-urban location in North-East India

B. Das* (1), B. Pathak(1, 2), L. Chutia(3), T. Subba(4), and P. K. Bhuyan(2)
(1) Department of Physics, Dibrugarh University 786004, Assam, India
(2) Center for Atmospheric Studies, Dibrugarh University 786004, Assam, India
(3) Department of Chemical and Biochemical Engineering, University of IOWA, USA
(4) Brookhaven National Laboratory, Upton, New York

Abstract

Atmospheric new particle formation (NPF) is generated through the secondary aerosol formation pathway, which enhances the total aerosol burden globally. Here we analyzed NPF events and their subsequent growth over Dibrugarh, in North-East India using a scanning mobility particle sizer (SMPS) during winter 2016. The occurrence of NPF is 15% of the days of observation. The rapid drop of geometric mean diameter (GMD) and simultaneously ultrafine particle concentration (N_{total}) burst in lower size segment designated the NPF burst and later continued to grow through coagulation and condensation with an average growth rate (GR) of 15.33 ± 5.50 nm/hr. Based on remote sensing observations (from OMI), the daily variation of NPF precursors such as NO_2, SO_2, and HCHO reveals that the concentration of these gases was higher than normal during the NPF days. The spatial distribution of NO_2 coupled with active fire count (from MODIS) reflects the dominance of NO_2 and, local fire events nearby the study site. The air mass back trajectories (HYSPLIT) confirm that the sources of emissions were confined within an area of ~100 km around Dibrugarh. These locally generated precursors, in conjunction with photochemistry, may be the cause of NPF occurrence at the study site. Long-term observation of the ultrafine particles to assess the seasonality of NPF events and simultaneous in-situ precursors that would provide better insight into NPF chemistry is planned in the immediate future.

1 Introduction

Understanding the total aerosol burden in the atmosphere is essential as it has an important role in weather, climate, public health, haze formation, and air quality [1, 2]. The aerosol population in the atmosphere is regulated by newly formed particles which are about 10-60% of the total, depending on the study site [3, 4, 5, 6]. Model simulations revealed that 50% of newly formed particles activate as cloud condensation nuclei (CCN) in the troposphere [7, 8, 9]. These newly created particles are formed through gaseous vapours that go through gas-to-particle (GTP) conversion and grow through coagulation scavenging and condensational growth [10]. High condensation growth leads to the large increment of a fraction of nucleation mode particles accumulated over the initially formed stable clusters, and pre-existing aerosols and coagulation are mainly attributed to size enhancement by collision and coalescence of aerosols present in the atmosphere [11, 12, 13]. NPF frequently occur in the continental boundary layer with a spatial and temporal scale of a few hundred kilometres, and 1-2 days respectively [14]. Several physicochemical mechanisms, including heterogeneous nucleation of organic insoluble vapours and chemical reactions, may initiate nucleated particle growth. The NPF dynamics are influenced by the type and amount of precursor vapours, the concentration of pre-existing particles, meteorological factors, and current atmospheric conditions [15]. Furthermore, charged ions clusters, organic acid, and their low-volatility compounds have the ability to initiate NPF [16]. Additionally, anthropogenic gaseous emissions oxidation products such as SO_2, NO_x, and VOC play an important role in NPF events, particularly in polluted marine environments [17, 18]. The distribution and fraction of secondary aerosols in total aerosol mass are highly uncertain, making it difficult to understand the impact of these aerosols on climate and health.

The present study aims to explore the characteristics of NPF, its growth mechanism and precursor dynamics integrating the ground- and space-based observation for the first time over Dibrugarh, a semi-urban location in North-East India.

2 Data and Methodology

2.1 Ground-based measurements

Particle size measurements were performed at Dibrugarh University (27.26°N, 94.53°E, 111m AMSL), Dibrugarh, which is located close to the North-Eastern boundary of India and experiences semi-urban, and subtropical climate [19].

The particle number size distribution (PNSD) was measured using the Scanning Mobility Particle Sizer (SMPS) with 97 size channels/bins starting from 10.2 nm

to 333.8 nm with a sample flow rate of 0.8 L/min and a Sheath flow rate of 8L/min.

2.2 Satellite observation

OMI and MODIS are NASA Earth Orbiting System (EOS) remote sensors used to study the dynamics of NPF precursors and active fire counts, respectively. The spatial distribution of tropospheric NO_2 from OMI data (0.25° × 0.25° resolution), and active fire counts from MODIS (1 km × 1 km) coupled with air mass trajectories (NOAA HYSPLIT trajectory model) were performed. The daily variation of NPF precursors such as tropospheric NO_2, total column SO_2, and total column HCHO was calculated.

2.3 Determination of particle growth rate (GR), geometric mean diameter (GMD)

The characterization of NPF events was based on the evaluation of several controlling processes. In this study, NPF events were identified by following the criteria set by Dal Maso and Kulmala [20]. The GR can be calculated by

$$GR = \frac{d(GMD)}{dt} \quad (1)$$

The log-normal size distribution for the observation of PNSD is of the following form [21],

$$\frac{dN}{d \ln D_p} = \sum_{i=1}^{n} \frac{N_i}{\sqrt{2\pi} \ln \sigma_{m,i}} \exp\left[\frac{(\ln D_p - \ln D_{m,p,i})^2}{2 \ln \sigma_{m,i}}\right] \quad (2)$$

Where, D_p is the particle diameter, n is the total number of modes, $D_{m,p,i}$ is the mode diameter in the i^{th} mode, $\sigma_{m,i}$ geometric standard deviation of the modes, and N_i is the number concentration of particles in i^{th} mode. The GMD for different particle modes can be evaluated by using [22],

$$GMD = \exp\left(\frac{1}{N} \sum n_i \times \ln D_i\right) \quad (3)$$

Where, D_i is the diameter of the i^{th} size bin.

3 Results and Discussion

3.1 Variation of number concentration (N_{total}), and geometric mean diameter (GMD)

We observed three NPF events during the winter 2016. Although, several NPF bursts were observed only those days, when the ultrafine particles size keeps on growing at a rate of a few nanometres per hour for a few hours at a stretch, are classified as growth event days [20]. A typical example of an NPF event on 3 December 2016 is considered as a representative day, where the nucleation burst was observed at 06:30 hrs (Figure 1a). The number concentration rapidly increases (N_{total} reached as high as ~ 3.96 × 10^4 cm^{-3}), and simultaneously dip in the GMD (GMD as low as ~ 48.05 nm) (Figure 1b). Later, the GMD value continues to increase with decreasing number concentration.

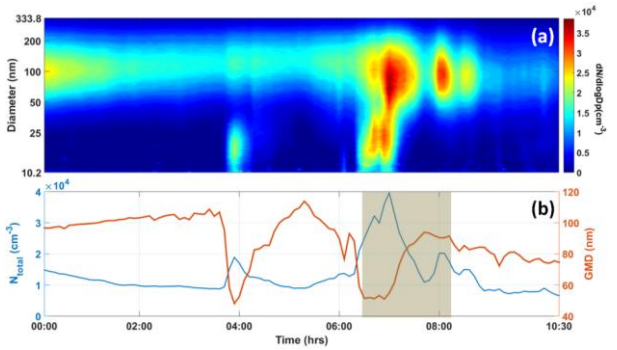

Figure 1. Representative observation of NPF event on 3 December 2016 (a) Contour plot of number concentration showing the formation and growth of new particles between 06:30 - 08:12 hrs and, (b) Variation of N_{total}, and GMD from midnight to 10:30 hrs, where the shaded portion is the event period.

3.2 Variation in different mode regimes

Figure 2 illustrates how the particles associated with GMD fluctuate under different mode regimes on the representative day 3 December 2016, where N_{nuc} in nucleation mode (D_p < 25 nm), N_{ait} in Aitken mode (25 ≤ D_p < 100 nm), and in N_{acc} accumulation mode (D_p ≥ 100 nm) [20]. During NPF days, the peaks occur in all regimes but the initial burst is seen in the nucleation mode, which later grew from nucleation to Aitken and then to accumulation mode. A large GMD dip occurs in the Aitken mode simultaneously with the nucleation burst in the nucleation mode, which supports the NPF burst.

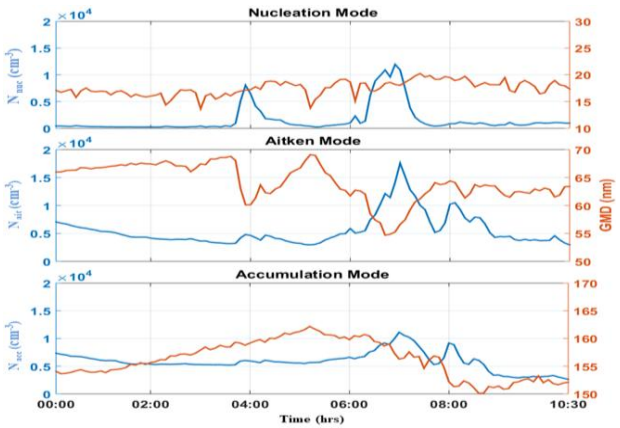

Figure 2. Variation of number concentration and GMD in three different modes: nucleation (top panel), Aitken (middle panel) and accumulation (bottom panel) on 3 December 2016 from midnight to 10:30 hrs.

3.3 Evolution of particle growth

The particle GR can be obtained by plotting the GMD of particle size distribution against time during the event period. The slope of the regression fit of the data for a certain time segment reveals the GR for that period. The GR was found to be 21 nm/hr on 3 December 2016 (Figure 3).

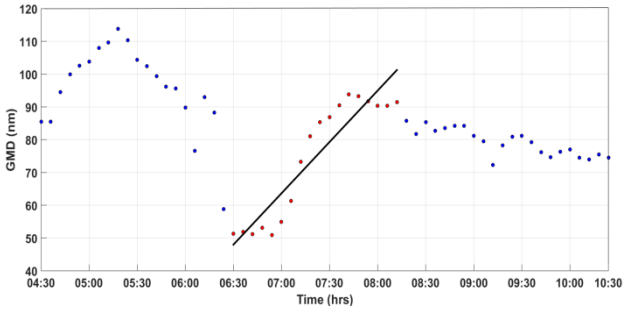

Figure 3. Scatter plot between the GMD versus local time. The solid line is the regression fit through GMD data points during the NPF growth period.

3.4 NPF precursor dynamics

The concentration of tropospheric NO_2 as well as the fire count in adjoining areas of the study location was significantly high (Figure 4). Moreover, to understand the possible flow path and source of transportation, air mass to the site, 48-hour backward trajectories (100 m, 500 m AGL) during the NPF period have been performed (Figure 4). The trajectories revealed confinement of the plumes within an area of ~100 km and traversing through the South-East part of the site where the maximum incidence of local fire events have been recorded.

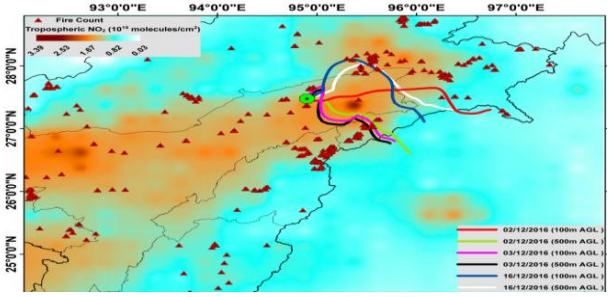

Figure 4. Map showing the distribution of tropospheric NO_2, and red triangles indicate the fires location from 15 November-16 December 2016. The solid colored lines represent the 48-hour air mass back trajectories, reaching the observation site on event days: 2 December (red and green), 3 December (purple and black) and 16 December (Blue and white), 2016.

The average concentration of NO_2, SO_2, and HCHO during the study period was found to be (9.76 ± 3.93) $\times 10^{15}$, (4.97 ± 5.35) $\times 10^{15}$, and (3.90 ± 2.91) $\times 10^{15}$ molecules/cm^2 respectively. During the NPF event days, the precursors' concentration level was higher than that of non-NPF days (Figure 5).

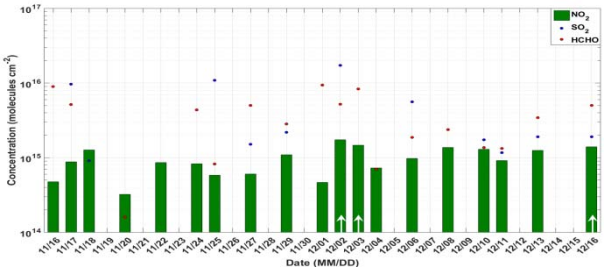

Figure 5. Daily variation of Tropospheric NO_2, total column SO_2 and HCHO during the study period (Arrow marks are the event days).

4 Summary and Conclusions

The NPF burst and their growth through the time derivative of GMD at a semi-urban location in the upper Brahmaputra basin in North-East India are investigated. The NPF occurrence frequency is found to be ~15%. The occurrence of NPF during daytime is primarily responsible for the photochemical process and that during night-time is likely due to the advection of precursors. A peak in number concentration with a simultaneous abrupt drop in GMD indicates an NPF burst with an abundance of ultrafine particles. We found the average growth rate was 15.33 ± 5.50 nm/hr on NPF days. The concentration of NPF precursors was high on NPF days. Moreover, from 48 hours air mass back trajectories at different AGL revealed that the plumes were locally confined. However, Long-term systematic observation of precursor gases and aerosols is required to understand the detailed NPF chemistry, seasonality and its contribution to total aerosol loading in relation to fog, haze, and cloud formation.

Acknowledgements

We acknowledge UGC for funding under SAP DRS II to procure the SMPS. Authors acknowledge the NASA GES-DISC for providing OMI and MODIS service for NO_2, SO_2, HCHO and active fire count data respectively, and the NOAA Air Resources Laboratory (ARL) for the provision of the HYSPLIT transport and/or READY website (https://www.ready.noaa.gov).

References

[1] R.-J. Huang *et al.*, "High secondary aerosol contribution to particulate pollution during haze events in China," *Nature*, vol. 514, no. 7521, pp. 218–222, Oct. 2014, doi: 10.1038/nature13774.

[2] V. P. Kanawade *et al.*, "What caused severe air pollution episode of November 2016 in New Delhi?," *Atmos. Environ.*, vol. 222, p. 117125, Feb. 2020, doi: 10.1016/j.atmosenv.2019.117125.

[3] C. Kuang, P. H. McMurry, and A. V. McCormick, "Determination of cloud condensation nuclei production from measured new particle formation events," *Geophys. Res. Lett.*, vol. 36, no. 9, p. L09822, May 2009, doi: 10.1029/2009GL037584.

[4] D. L. Yue *et al.*, "Potential contribution of new particle formation to cloud condensation nuclei in Beijing," *Atmos. Environ.*, vol. 45, no. 33, pp. 6070–6077, Oct. 2011, doi: 10.1016/j.atmosenv.2011.07.037.

[5] C. Rose *et al.*, "CCN production by new particle formation in the free troposphere," *Atmospheric Chem. Phys.*, vol. 17, no. 2, pp. 1529–1541, Jan. 2017, doi: 10.5194/acp-17-1529-2017.

[6] V.-M. Kerminen, X. Chen, V. Vakkari, T. Petäjä, M. Kulmala, and F. Bianchi, "Atmospheric new particle formation and growth: review of field observations," *Environ. Res. Lett.*, vol. 13, no. 10, p. 103003, Sep. 2018, doi: 10.1088/1748-9326/aadf3c.

[7] D. V. Spracklen, K. S. Carslaw, M. Kulmala, V.-M. Kerminen, G. W. Mann, and S.-L. Sihto, "The contribution of boundary layer nucleation events to total particle concentrations on regional and global scales," *Atmospheric Chem. Phys.*, vol. 6, no. 12, pp. 5631–5648, Dec. 2006, doi: 10.5194/acp-6-5631-2006.

[8] J. Merikanto, D. V. Spracklen, G. W. Mann, S. J. Pickering, and K. S. Carslaw, "Impact of nucleation on global CCN," *Atmospheric Chem. Phys.*, vol. 9, no. 21, pp. 8601–8616, Nov. 2009, doi: 10.5194/acp-9-8601-2009.

[9] H. Gordon *et al.*, "Causes and importance of new particle formation in the present-day and preindustrial atmospheres: CAUSES AND ROLE OF NEW PARTICLE FORMATION," *J. Geophys. Res. Atmospheres*, vol. 122, no. 16, pp. 8739–8760, Aug. 2017, doi: 10.1002/2017JD026844.

[10] M. Kulmala, L. Pirjola, and J. M. Mäkelä, "Stable sulphate clusters as a source of new atmospheric particles," *Nature*, vol. 404, no. 6773, pp. 66–69, Mar. 2000, doi: 10.1038/35003550.

[11] P. H. McMurry and S. K. Friedlander, "New particle formation in the presence of an aerosol," *Atmospheric Environ. 1967*, vol. 13, no. 12, pp. 1635–1651, Jan. 1979, doi: 10.1016/0004-6981(79)90322-6.

[12] M. Kulmala, K. E. J. Lehtinen, and A. Laaksonen, "Cluster activation theory as an explanation of the linear dependence between formation rate of 3nm particles and sulphuric acid concentration," *Atmospheric Chem. Phys.*, vol. 6, no. 3, pp. 787–793, Mar. 2006, doi: 10.5194/acp-6-787-2006.

[13] P. H. McMurry *et al.*, "A criterion for new particle formation in the sulfur-rich Atlanta atmosphere," *J. Geophys. Res.*, vol. 110, no. D22, p. D22S02, 2005, doi: 10.1029/2005JD005901.

[14] M. Kulmala *et al.*, "Measurement of the nucleation of atmospheric aerosol particles," *Nat. Protoc.*, vol. 7, no. 9, pp. 1651–1667, Sep. 2012, doi: 10.1038/nprot.2012.091.

[15] F. Raes, "Entrainment of free tropospheric aerosols as a regulating mechanism for cloud condensation nuclei in the remote marine boundary layer," *J. Geophys. Res.*, vol. 100, no. D2, p. 2893, 1995, doi: 10.1029/94JD02832.

[16] J. Kirkby *et al.*, "Role of sulphuric acid, ammonia and galactic cosmic rays in atmospheric aerosol nucleation," *Nature*, vol. 476, no. 7361, pp. 429–433, Aug. 2011, doi: 10.1038/nature10343.

[17] E. D. Bates, R. D. Mayton, I. Ntai, and J. H. Davis, "CO_2 Capture by a Task-Specific Ionic Liquid," *J. Am. Chem. Soc.*, vol. 124, no. 6, pp. 926–927, Feb. 2002, doi: 10.1021/ja017593d.

[18] C. D. O'Dowd and T. Hoffmann, "Coastal New Particle Formation: A Review of the Current State-Of-The-Art," *Environ. Chem.*, vol. 2, no. 4, p. 245, 2005

[19] B. Pathak, L. Chutia, C. Bharali, and P. K. Bhuyan, "Continental export efficiencies and delineation of sources for trace gases and black carbon in North-East India: Seasonal variability," *Atmos. Environ.*, vol. 125, pp. 474–485,Jan. 2016, doi: 10.1016/j.atmosenv.2015.09.020.

[20] M. Dal Maso *et al.*, "Formation and growth of fresh atmospheric aerosols: eight years of aerosol size distribution data from SMEAR II, Hyytiälä, Finland" *BOREAL Environ. Res.*,10, pp. 323–336, 2005.

[21] J. H. Seinfeld and S. N. Pandis, "*Atmospheric Chemistry and Physics: From Air Pollution to Climate Change*," 2nd Edition. John Wiley & Sons, New York, 2006.

[22] W. C. Hinds, "*Aerosol Technology: Properties, Behavior, and Measurements of Airborne Particles*," John Wiley & Sons, INC., New York, 1998.